The timelike Compton scattering at high and medium energies

Lech Szymanowski

National Centre for Nuclear Research (NCBJ),
Warsaw, Poland

in collaboration with
B. Pire (CPhT, Palaiseau) and J. Wagner (NCBJ, Warsaw)

Phys.Rev.D79:014010 (2009), Phys.Rev.D83:034009 (2011)

Frontiers in QCD (INT-11-3), September 19 - November 18, 2011

Motivation

In 80's, lot of studies of INCLUSIVE:

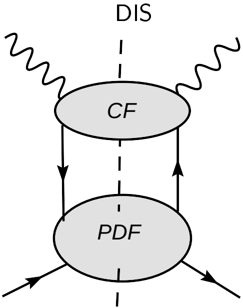

versus

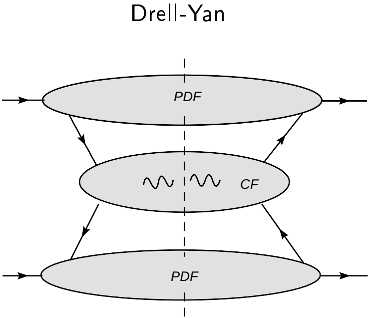

- parton model from QCD factorization
- $\mathrm{CF}_{DIS}(q^2 < 0)$ with SPACELIKE γ^* versus
  $\mathrm{CF}_{DY}(q^2 > 0)$ with TIMELIKE γ^*
- at NLO order: 1-loop corrections to $\mathrm{CF}_{DY}(q^2 > 0)$ are very big

  necessity of resummation to all orders before comparison with data

Motivation

Now: intensive studies of EXCLUSIVE processes

- Deeply Virtual C ompton Scattering (DVCS) with $q^2 < 0$, i.e. with SPACELIKE γ^*

  high energies: DESY: H1 and ZEUS; EIC

  medium energies: HERMES, JLAB

- within ongoing, accepted and planned Drell-Yan (DY) programs with $q^2 > 0$, i.e. with TIMELIKE γ^*

  high energies: ultraperipheral scattering at LHC and RHIC, COMPASS

  medium energies: HERMES, JLAB@12GeV, GSI-FAIR

Motivation

Two phenomenologically important EXCLUSIVE processes:

DVCS versus Timelike Compton Scattering (TCS)

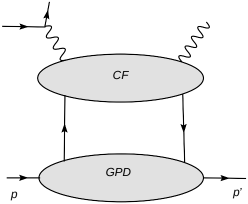

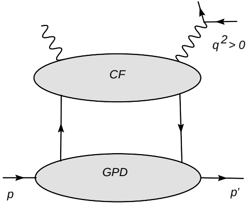

- QCD factorization with Generalized Parton Distributions (GPDs)
- $\mathrm{CF}_{DVCS}(q^2 < 0)$ known at NLO since 98 — Mankiewicz et al, Belitsky et al
- $\mathrm{CF}_{TCS}(q^2 > 0)$ at NLO derived in 2011 — B. Pire et al Phys. Rev. D83
- resummation of large contributions in EXCLUSIVE processes — in progress

Motivation

Additional phenomenologically important EXCLUSIVE process:
Double Deeply Virtual Compton Scattering (DDVCS)

Guidal et al Phys. Rev. Lett. 90 (2003)

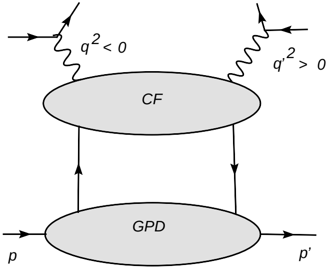

- analysis started by HERMES, soon in JLab
- $\mathrm{CF}_{DDVCS}(q^2 > 0)$ at NLO derived in 2011 B. Pire et al Phys. Rev. D83

Kinematics of TCS

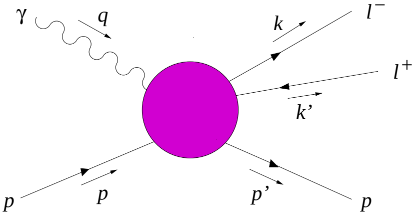

Figure: Real photon-proton scattering into a lepton pair and a proton.

$$\gamma(q)N(p) \to \gamma^*(q')N(p') \to l^-(k)l^+(k')N(p')$$

at small $t = (p' - p)^2$ and large *timelike* virtuality $(k + k')^2 = q'^2 = Q'^2$ of the final state dilepton

Experiments:

- high energies: at LHC, RHIC — small-x physics as ultraperipheral scattering (with B-W real γ's)
- lower energies: JLab

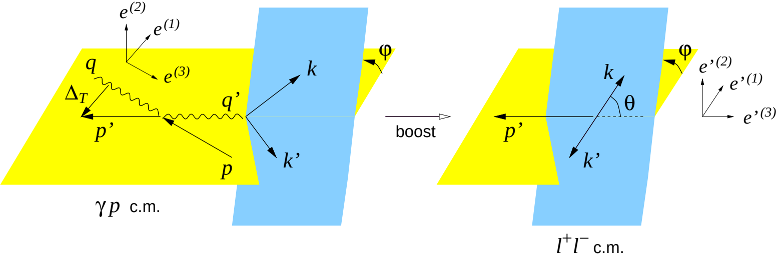

Figure: Kinematical variables and coordinate axes in the γp and $\ell^+\ell^-$ c.m. frames.

The Bethe-Heitler contribution

purely electromagnetic contribution

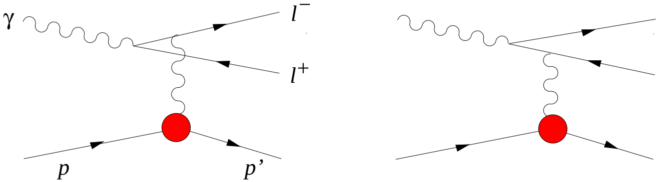

Figure: The Feynman diagrams for the Bethe-Heitler amplitude.

$$\frac{d\sigma_{BH}}{dQ'^2\,dt\,d(\cos\theta)\,d\varphi} \approx \frac{\alpha_{em}^3}{2\pi s^2}\,\frac{1}{-t}\,\frac{1+\cos^2\theta}{\sin^2\theta}\left[\left(F_1^2 - \frac{t}{4M^2}F_2^2\right)\frac{2}{\tau^2}\,\frac{\Delta_T^2}{-t} + (F_1+F_2)^2\right]$$

For small θ BH contribution becomes very large

The Compton contribution

Born contribution

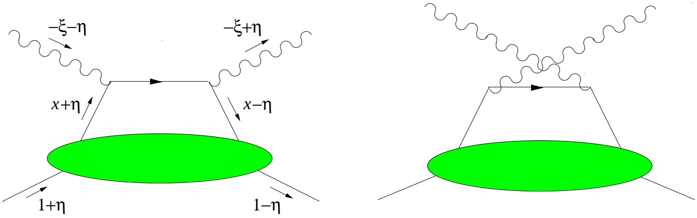

Figure: Handbag diagrams for the Compton process in the scaling limit. The plus-momentum fractions x, ξ, η refer to the average proton momentum $\frac{1}{2}(p+p')$.

$$x = \frac{(k+k')^+}{(p+p')^+},\ \xi \approx -\frac{(q+q')^+}{(p+p')^+},\ \eta \approx \frac{(p-p')^+}{(p+p')^+}.$$

To leading-twist accuracy one has $\xi = -\eta = -\tau/(2-\tau)$, where $\tau = Q'^2/s$ is Björken variable.

Quark (unpolarised) GPDs:

$$
\begin{aligned}
F^q &= \frac{1}{2}\int \frac{dz^-}{2\pi} e^{ixP^+z^-} \langle p'|\bar{q}(-\frac{1}{2}z)\gamma^+ q(\frac{1}{2}z)|p\rangle|_{z^+=0,\,\mathbf{z}=0} \\
&= \frac{1}{2P^+}\left[H^q(x,\eta,t)\bar{u}(p')\gamma^+ u(p) + E^q(x,\eta,t)\bar{u}(p')\frac{i\sigma^{+\,\alpha}\Delta_\alpha}{2m}u(p)\right]
\end{aligned}
$$

Gluon (unpolartized) GPDs:

$$
\begin{aligned}
F^g &= \frac{1}{P^+}\int \frac{dz^-}{2\pi} e^{ixP^+z^-} \langle p'|G^{+\,\mu}(-\frac{1}{2}z)G_\mu^{\ +}(\frac{1}{2}z)|p\rangle|_{z^+=0,\,\mathbf{z}=0} \\
&= \frac{1}{2P^+}\left[H^g(x,\eta,t)\bar{u}(p')\gamma^+ u(p) + E^g(x,\eta,t)\bar{u}(p')\frac{i\sigma^{+\,\alpha}\Delta_\alpha}{2m}u(p)\right]
\end{aligned}
$$

the Compton form factors:

$$\begin{aligned}
\mathcal{H}_1(\xi,\eta,t) &= \sum_q e_q^2 \int_{-1}^{1} dx \Big(\frac{1}{\xi - x - i\epsilon} - \frac{1}{\xi + x - i\epsilon} \Big) H^q(x,\eta,t), \\
\mathcal{E}_1(\xi,\eta,t) &= \sum_q e_q^2 \int_{-1}^{1} dx \Big(\frac{1}{\xi - x - i\epsilon} - \frac{1}{\xi + x - i\epsilon} \Big) E^q(x,\eta,t), \\
\tilde{\mathcal{H}}_1(\xi,\eta,t) &= \sum_q e_q^2 \int_{-1}^{1} dx \Big(\frac{1}{\xi - x - i\epsilon} + \frac{1}{\xi + x - i\epsilon} \Big) \tilde{H}^q(x,\eta,t), \\
\tilde{\mathcal{E}}_1(\xi,\eta,t) &= \sum_q e_q^2 \int_{-1}^{1} dx \Big(\frac{1}{\xi - x - i\epsilon} + \frac{1}{\xi + x - i\epsilon} \Big) .\tilde{E}^q(x,\eta,t)
\end{aligned}$$

For example: $M^{\lambda' \lambda^{\gamma^*}, \lambda \lambda^{\gamma}}$

$$M^{+-,+-}\Big|_{TCS} =$$

$$\sqrt{1-\eta^2}\Big(\mathcal{H}_1(-\eta,\eta,t) + \tilde{\mathcal{H}}_1(-\eta,\eta,t) - \frac{\eta^2}{1-\eta^2}\big(\mathcal{E}_1(-\eta,\eta,t) + \tilde{\mathcal{E}}_1(-\eta,\eta,t)\big)\Big)$$

Modelizing GPDs for Ultraperipheral Collisions (UPC) small-x

Factorized ansatz for t-dependence:

$$\begin{aligned} H^u(x,\eta,t) &= h^u(x,\eta)\frac{1}{2}F_1^u(t) \\ H^d(x,\eta,t) &= h^d(x,\eta)F_1^d(t) \\ H^s(x,\eta,t) &= h^s(x,\eta)F_D(t) \end{aligned}$$

Double distribution ansatz for h^q without any D-term:

$$\begin{aligned} h^q(x,\eta) &= \int_0^1 dx' \int_{-1+x'}^{1-x'} dy' \\ &\quad \Big[\delta(x-x'-\eta y')q(x') - \delta(x+x'-\eta y')\bar{q}(x')\Big]\pi(x',y') \\ \pi(x',y') &= \frac{3}{4}\frac{(1-x')^2 - y'^2}{(1-x')^3} \end{aligned}$$

For the unpolarized distributions $q(x)$ and $\bar{q}(x)$ we take NLO($\overline{\mathrm{MS}}$) GRVGJR 2008 parametrization.

They have strong dependence of the factorization scale choice for small x:

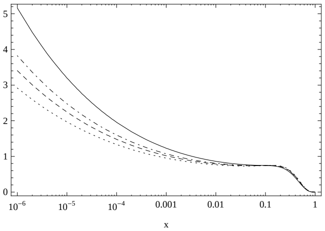

Figure: The NLO($\overline{MS}$) GRVGJR 2008 parametrization of $u(x) + \bar{u}(x)$ for different factorization scales $\mu_F^2 = 4$ (dotted) , 5 (dashed) , 6 (dash-dotted) , 10 (solid) GeV^2.

This results in the strong dependence of h^q for small values of η:

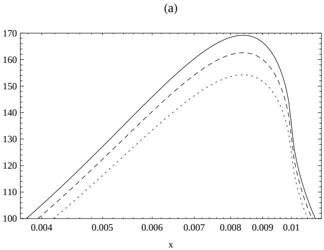

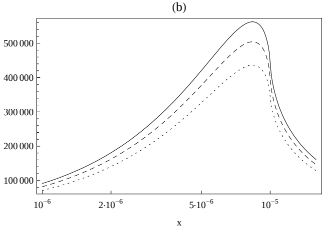

Figure: $h_+^u(x,\eta) = h^u(x,\eta) - h^u(-x,\eta)$ for $\eta = 10^{-2}$ (a) and for $\eta = 10^{-5}$ (b) for different factorization scales $\mu_F^2 = 4$ (dotted) , 5 (dashed) , 6 (solid) GeV^2.

B-H cross section at UPC

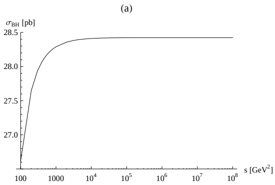

Figure: (a) The BH cross section integrated over $\theta \in [\pi/4, 3\pi/4]$, $\varphi \in [0, 2\pi]$, $Q'^2 \in [4.5, 5.5]\,\mathrm{GeV}^2$, $|t| \in [0.05, 0.25]\,\mathrm{GeV}^2$, as a function of γp c.m. energy squared s. (b) The BH cross section integrated over $\varphi \in [0, 2\pi]$, $|t| \in [0.05, 0.25]\,\mathrm{GeV}^2$, and various ranges of θ : $[\pi/3, 2\pi/3]$ (dotted), $[\pi/4, 3\pi/4]$ (dashed) and $[\pi/6, 5\pi/6]$ (solid), as a function of Q'^2 for $s = 10^5\,\mathrm{GeV}^2$

TCS cross section at UPC

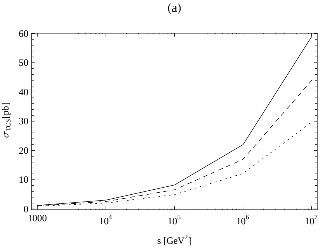

Figure: σ_{TCS} as a function of γp c.m. energy squared s, for GRVGJR2008 LO (a) and NLO (b) parametrizations, for different factorization scales $\mu_F^2 = 4$ (dotted), 5 (dashed), 6 (solid) GeV^2.

For very high energies σ_{TCS} calculated with $\mu_F^2 = 6\,\mathrm{GeV}^2$ is much bigger then with $\mu_F^2 = 4\,\mathrm{GeV}^2$. Also predictions obtained using LO and NLO GRVGJR2008 PDFs differ significantly.

The interference cross section at UPC

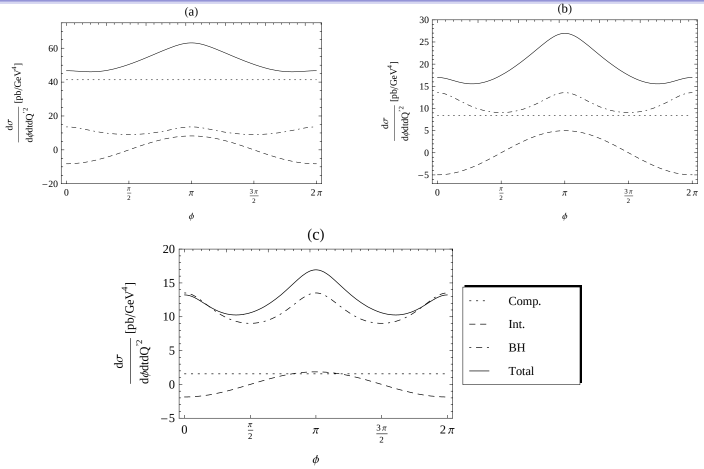

Figure: The differential cross sections (solid lines) for $t = -0.2\,\mathrm{GeV}^2$, $Q'^2 = 5\,\mathrm{GeV}^2$ and integrated over $\theta = [\pi/4, 3\pi/4]$, as a function of φ, for $s = 10^7\,\mathrm{GeV}^2$ (a), $s = 10^5\,\mathrm{GeV}^2$(b), $s = 10^3\,\mathrm{GeV}^2$ (c) with $\mu_F^2 = 5\,\mathrm{GeV}^2$. We also display the Compton (dotted), Bethe-Heitler (dash-dotted) and Interference (dashed) contributions.

Rate estimates for UPC

$$\sigma_{pp} = 2\int \frac{dn(k)}{dk}\sigma_{\gamma p}(k)dk$$

$\sigma_{\gamma p}(k)$ is the cross section for the $\gamma p \to p l^+ l^-$ process and k is the γ's energy.

$\frac{dn(k)}{dk}$ is an equivalent photon flux

$$\frac{dn(k)}{dk} = \frac{\alpha}{2\pi k}\left[1+(1-\frac{2k}{\sqrt{s_{pp}}})^2\right]\left(\ln A - \frac{11}{6} + \frac{3}{A} - \frac{3}{2A^2} + \frac{1}{3A^3}\right)$$

$A = 1 + \frac{0.71\,\mathrm{GeV}^2}{Q^2_{min}}$, $Q^2_{min} \approx \frac{4M_p^2 k^2}{s_{pp}}$ is the minimal $-t$
s_{pp} is the proton-proton energy squared ($\sqrt{s_{pp}} = 14\,\mathrm{TeV}$): $s \approx 2\sqrt{s_{pp}}k$

The pure Bethe - Heitler contribution to σ_{pp}, integrated over $\theta = [\pi/4, 3\pi/4]$, $\phi = [0, 2\pi]$, $t = [-0.05\,\mathrm{GeV}^2, -0.25\,\mathrm{GeV}^2]$, $Q'^2 = [4.5\,\mathrm{GeV}^2, 5.5\,\mathrm{GeV}^2]$, and photon energies $k = [20, 900]\,\mathrm{GeV}$ gives:

$$\sigma_{pp}^{BH} = 2.9\text{pb} .$$

The Compton contribution (calculated with NLO GRVGJR2008 PDFs, and $\mu_F^2 = 5\,\mathrm{GeV}^2$) gives:

$$\sigma_{pp}^{TCS} = 1.9\text{pb} .$$

LHC: rate $\sim 10^5$ events/year with nominal luminosity (10^{34} cm^{-2}s^{-1})

TCS at lower energies

Berger, Diehl, Pire, 2002

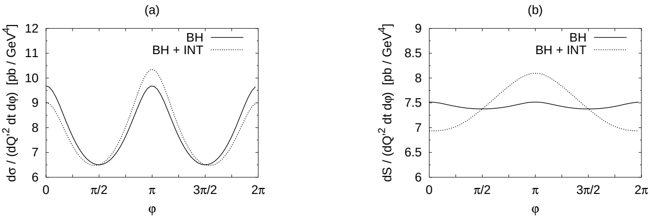

Figure:

B-H dominant; TCS dominated by quark GPDs

Charge asymmetry $\sim$ interference of B-H and TCS

TCS at lower energies

NLO corrections necessary:

$$R = \frac{\int d\phi \ \cos(\phi) d\sigma}{\int d\phi \ d\sigma}$$

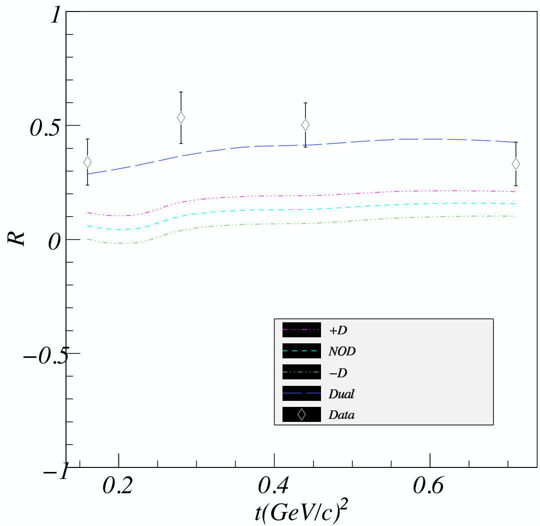

NLO corrections

$$\gamma^*(q_{in})N \to \gamma^*(q_{out})N'$$

DVCS versus TCS versus DDVCS:

- DVCS: $q_{in}^2 < 0\,, \quad q_{out}^2 = 0$
- TCS: $q_{in}^2 = 0\,, \quad q_{out}^2 > 0$
- DDVCS: $q_{in}^2 < 0\,, \quad q_{out}^2 > 0$

Why NLO corrections of TCS are interested:

- at high energies gluons important, they enter at NLO
- DIS versus Drell-Yan: big K-factors $\quad \log\frac{-Q^2}{\mu_F^2} \to \log\frac{Q^2}{\mu_F^2} \pm i\pi$
- dependence (strong ?? or weak ??) on the factorization scale μ_F
- DVCS$_{unphysicalregion}$ $\quad \xi \to \xi - i\varepsilon \quad$ DVCS$_{physicalregion}$

in TCS and DDVCS it is not enough

Kinematics in Ji's (symmetric) notation

incoming photon $q_{in} = (q - \xi p)$
incoming proton $P = (1 + \xi)p$

outgoing photon $(q_{out} = q + \xi p)$
outgoing proton $P' = (1 - \xi)p$

$$
\begin{aligned}
p &= p^+(1,0,0,1)\,, \\
n &= \frac{1}{2p^+}(1,0,0,-1)\,, \\
q &= -x_B p + \frac{Q^2}{2x_B} n
\end{aligned}
$$

so: $pn = 1$, $s = (p+q)^2 = \frac{1-x_B}{x_B} Q^2$ and $x_B = \frac{Q^2}{s+Q^2}$

$$
q_{in}^2 = -Q^2(1 + \frac{\xi}{x_B}) \quad q_{out}^2 = -Q^2(1 - \frac{\xi}{x_B})
$$

DVCS: $x_B = \xi$, $Q^2 > 0$

TCS: $x_B = -\xi$, $Q^2 = -Q'^2 < 0$

DDVCS: $0 < x_B < \xi$ and $Q^2 > 0$ OR $0 > x_B > -\xi$ and $Q^2 < 0$

Amplitude:

$$\mathcal{A}^{\mu\nu} = g_T^{\mu\nu} \int_{-1}^{1} dx \left[\sum_q^{n_F} T^q(x) F^q(x) + T^g(x) F^g(x) \right]$$

where renormalized coefficient functions are given by:

$$\begin{aligned} T^q &= C_0^q + C_1^q + \frac{1}{2} \ln\left(\frac{|Q^2|}{\mu_F^2} \right) \cdot C_{coll}^q \,, \\ T^g &= C_1^g + \frac{1}{2} \ln\left(\frac{|Q^2|}{\mu_F^2} \right) \cdot C_{coll}^g \end{aligned}$$

and the GPDs are

$$\begin{aligned} F^q(x,\xi) &= \frac{1}{2} \int \frac{d\lambda}{2\pi} e^{-i\lambda x} \left\langle P' \middle| \bar{\psi}_q \left(\frac{\lambda}{2} n \right) \gamma^\mu \psi_q \left(-\frac{\lambda}{2} n \right) \middle| P \right\rangle n_\mu \,, \\ F^g(x,\xi) &= -\frac{1}{2x} \int \frac{d\lambda}{2\pi} e^{-i\lambda x} \left\langle P' \middle| G_a^{\mu\alpha} \left(\frac{\lambda}{2} n \right) G_{a\alpha}^{\nu} \left(-\frac{\lambda}{2} n \right) \middle| P \right\rangle n_\mu n_\nu \end{aligned}$$

Diagrams

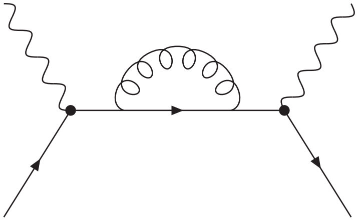

Figure: Self energy correction to $q\gamma \rightarrow q\gamma$ scattering amplitude

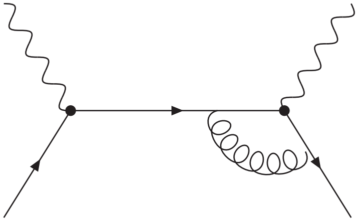

Figure: Right vertex correction to $q\gamma \to q\gamma$ scattering amplitude

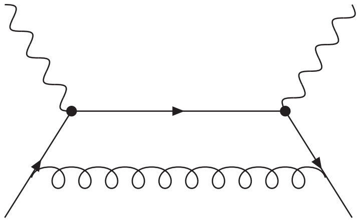

Figure: Box diagram correction to $q\gamma \to q\gamma$ scaterring amplitude

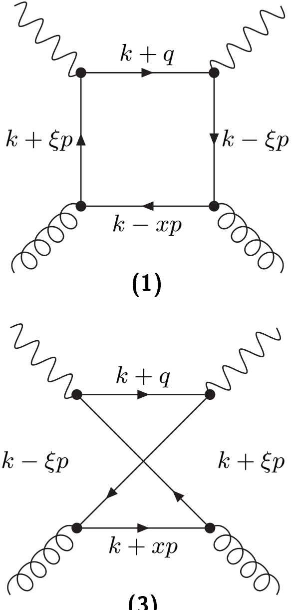

Figure: First group of diagrams describing $\gamma g \to \gamma g$ scattering.

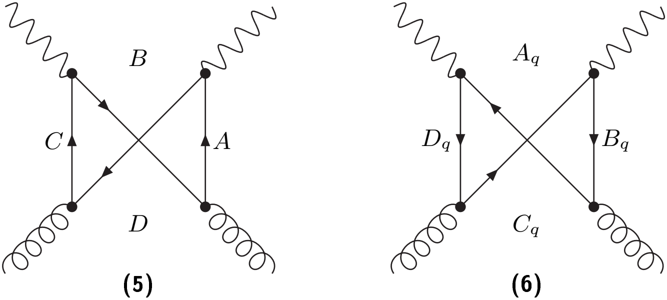

Figure: Second group of diagrams describing $\gamma g \to \gamma g$ scattering.

Results: TCS + DVCS + DDVCS

TCS:
Quark coefficient functions:

$$C_0^q = e_q^2 \left(\frac{1}{x-\xi-i\varepsilon} + \frac{1}{x+\xi+i\varepsilon} \right) ,$$

$$C_1^q = \frac{e_q^2 \alpha_S C_F}{4\pi}$$

$$\left\{ \frac{1}{x-\xi-i\varepsilon} \left[-9 + 3\log(-1+\frac{x}{\xi}-i\varepsilon) - 6\frac{\xi}{x+\xi}\log(-1+\frac{x}{\xi}-i\varepsilon) + 6\frac{\xi}{x+\xi}\log(-2-i\varepsilon) \right.\right.$$
$$\left. + \log^2(-1+\frac{x}{\xi}-i\varepsilon) - \log^2(-2-i\varepsilon) \right]$$
$$+ \frac{1}{x+\xi+i\varepsilon} \left[-9 + 3\log(-1-\frac{x}{\xi}-i\varepsilon) + 6\frac{\xi}{x-\xi}\log(-1-\frac{x}{\xi}-i\varepsilon) - 6\frac{\xi}{x-\xi}\log(-2-i\varepsilon) \right.$$
$$\left.\left. + \log^2(-1-\frac{x}{\xi}-i\varepsilon) - \log^2(-2-i\varepsilon) \right] \right\} ,$$

$$C_{coll}^q = \frac{e_q^2 \alpha_S C_F}{4\pi} \left\{ \frac{1}{x-\xi-i\varepsilon} \left[6 + 4\log(-1+\frac{x}{\xi}-i\varepsilon) - 4\log(-2-i\varepsilon) \right] \right.$$
$$\left. + \frac{1}{x+\xi+i\varepsilon} \left[6 + 4\log(-1-\frac{x}{\xi}-i\varepsilon) - 4\log(-2-i\varepsilon) \right] \right\}$$

Gluon coefficient functions:

$$C^g_{coll} = \frac{\left(\sum_q e_q^2\right)\alpha_S T_F}{4\pi} \frac{8x}{(x+\xi+i\varepsilon)(x-\xi-i\varepsilon)} \cdot$$
$$\left[\frac{x-\xi}{x+\xi}\log\left(-1+\frac{x}{\xi}-i\varepsilon\right)+\frac{x+\xi}{x-\xi}\log\left(-1-\frac{x}{\xi}-i\varepsilon\right)-2\frac{x^2+\xi^2}{x^2-\xi^2}\log(-2-i\varepsilon)\right],$$

$$\begin{aligned} C^g_1 = {} & \frac{\left(\sum_q e_q^2\right)\alpha_S T_F}{4\pi} \frac{2x}{(x+\xi+i\varepsilon)(x-\xi-i\varepsilon)} \cdot \\ & \left[-2\frac{x-3\xi}{x+\xi}\log\left(-1+\frac{x}{\xi}-i\varepsilon\right)+\frac{x-\xi}{x+\xi}\log^2\left(-1+\frac{x}{\xi}-i\varepsilon\right)\right. \\ & -2\frac{x+3\xi}{x-\xi}\log\left(-1-\frac{x}{\xi}-i\varepsilon\right)+\frac{x+\xi}{x-\xi}\log^2\left(-1-\frac{x}{\xi}-i\varepsilon\right) \\ & \left.+4\frac{x^2+3\xi^2}{x^2-\xi^2}\log(-2-i\varepsilon)-2\frac{x^2+\xi^2}{x^2-\xi^2}\log^2(-2-i\varepsilon)\right] \end{aligned}$$

Discussion

- DVCS: the imaginary parts from $\xi \to \xi - i\varepsilon$
- TCS:
  - part of imaginary parts from $\xi \to \xi + i\varepsilon$
  - there appear e.g. $\log^2(-2 - i\varepsilon)$ which contribute to imaginary parts
  - in DVCS the imaginary part are in DGLAP region
    in TCS they are in DGLAP AND ERBL
- at LO: $C^q_{0(DVCS)} = {C^q_{0(TCS)}}^*$

  at NLO: $C^q_{coll(DVCS)} = {C^q_{coll(TCS)}}^*$ and $C^g_{coll(DVCS)} = {C^g_{coll(TCS)}}^*$

NLO quark:

$$\frac{{C^q_{1(TCS)}}^* - C^q_{1(DVCS)}}{\frac{e^2\alpha_S C_F}{4\pi}} =$$

$$\frac{1}{x-\xi+i\varepsilon}\left[\left(3-2\log 2+2\log|1-\frac{x}{\xi}|\right)(i\pi)+\pi^2\left(1+\theta(x-\xi)-\theta(-x+\xi)\right)\right]$$

$$+\frac{1}{x+\xi-i\varepsilon}\left[\left(3-2\log 2+2\log|1+\frac{x}{\xi}|\right)(i\pi)+\pi^2\left(1+\theta(-x-\xi)-\theta(x+\xi)\right)\right]$$

NLO gluon in DGLAP region:

$$\frac{C^g_{1(TCS)} - C^g_{1(DVCS)}}{\frac{\left(\sum_q e_q^2\right)\alpha_S T_F}{4\pi}} \overset{x\geq\xi}{=} \frac{2x}{x^2-\xi^2}\left[2\frac{x-\xi}{x+\xi}\pi^2\right.$$

$$\left.+\left(-4\frac{x-3\xi}{x+\xi}+2\frac{x-\xi}{x+\xi}\log|1-\frac{x}{\xi}|-2\frac{x+\xi}{x-\xi}\log|1+\frac{x}{\xi}|+4\frac{x^2+\xi^2}{x^2-\xi^2}\log 2\right)(-i\pi)\right]$$

$$\text{quark ratio:} \quad R^q = \frac{C_1^q + \frac{1}{2}\log\left(\frac{|Q^2|}{\mu_F^2}\right) \cdot C_{coll}^q}{C_0^q}$$

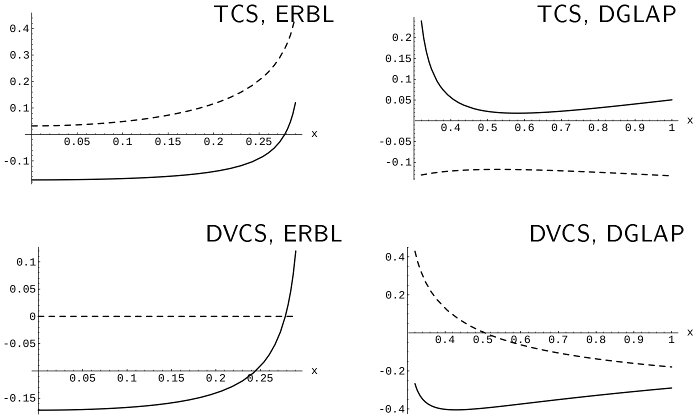

Figure: Real (solid line) and imaginary (dashed line) part of the ratio R^q of the NLO quark coefficient function to the Born term in Timelike Compton Scattering (up) and Deeply Virtual Compton Scattering (down) as a function of x in the ERBL (left) and DGLAP (right) region for $\xi = 0.3$, for $\mu_F^2 = |Q^2|$.

another quark ratio: $R^q_{T-S} = \dfrac{C^q_{1(TCS)} - C^{q\,*}_{1(DVCS)}}{C^q_0}$

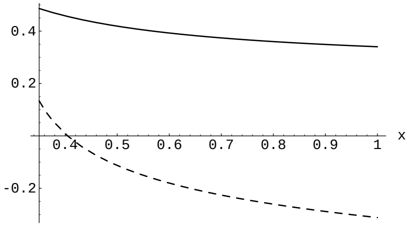

Figure: Real (solid line) and imaginary (dashed line) part of the ratio R^q_{T-S} of difference of NLO quark coefficient functions to the LO coefficient functions in the TCS and DVCS as a function of x in the DGLAP region for $\xi = 0.3$.

gluonic ratios:

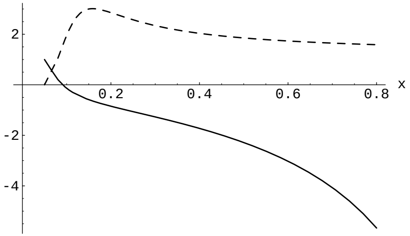

Figure: Ratio of the real (solid line) and imaginary (dashed line) part of the NLO gluon coefficient function in TCS to the same quantity in DVCS as a function of x in the DGLAP region for $\xi = 0.05$ for $\mu_F^2 = |Q^2|$.

Factorisation scale dependence of quark CF:

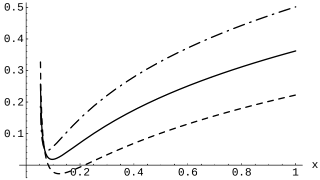

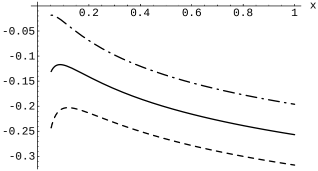

Figure: Factorization scale dependence of the real (left) and imaginary (right) parts of ratio R^q of NLO quark correction to hard scattering amplitudes to Born level coefficient function of the Timelike Compton Scattering as a function of x in the DGLAP region for $\xi = 0.05$. The ratios are plotted for the values of $\frac{|Q^2|}{\mu_F^2}$ equal 0.5 (dashed), 1 (solid) and 2 (dash-dotted line).

Factorisation scale dependence of gluonic CF:

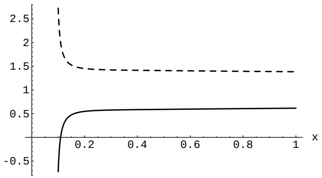

Figure: Ratios of the real (left) and imaginary (right) parts of NLO gluon coefficient function for $|Q^2| = 1/2\mu_F^2$ (solid line) and $|Q^2| = 2\mu_F^2$ (dashed line) to the same quantities with $|Q^2| = \mu_F^2$. Those quantities are calculated for the timelike Compton scattering and plotted as a function of x in the DGLAP region for $\xi = 0.05$.

Estimates for DVCS

ξ dependence of Compton form factors for DVCS with GPDs obtained from double distribution

solid line: LO Re H_u
dotted line: LO Im H_u
dashed line: Full NLO Re H_u
dot-dashed line: Full NLO Im H_u

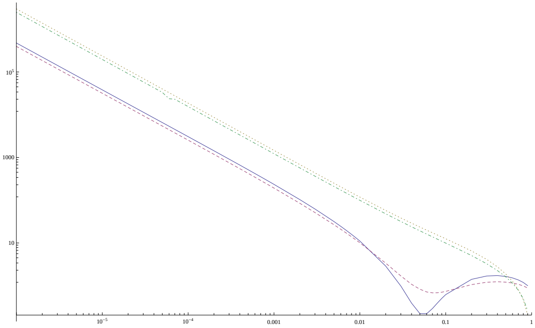

Figure: Double distr. with PDF by Goloskokov-Kroll for $Q^2 = 4\text{GeV}^2$, $\mu_F = Q$ and $t = 0$

Estimates for DVCS cntd

ξ dependence of Compton form factors for DVCS with GPDs obtained from double distribution

solid line: LO Re H_u
dotted line: LO Im H_u dashed line: Full NLO Re H_u
dot-dashed line: Full NLO Im H_u

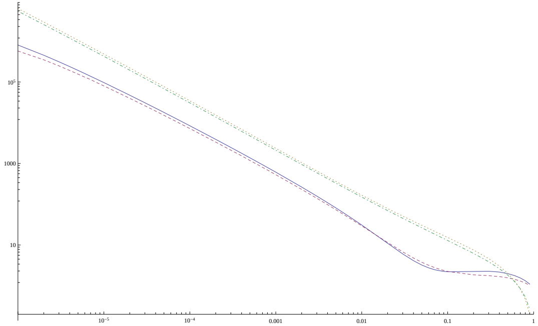

Figure: Double distr. with PDF by MSTW for $Q^2 = 4\mathrm{GeV}^2$, $\mu_F = Q$ and $t = 0$

Estimates for DVCS cntd

ξ dependence of Compton form factors for DVCS with GPDs obtained from double distribution obtained with MSTW PDFs

$$CFF = LO \;+\; NLO \qquad \text{Ratio} = \frac{NLO}{LO}$$

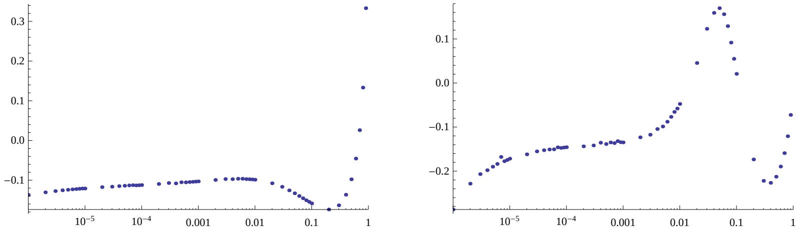

Figure: Ratios of NLO correction to Born contribution for imaginary (left figure) and real (right figure) parts for $Q^2 = 4\text{GeV}^2$, $\mu_F = Q$, $t = 0$

Estimates for TCS

ξ dependence of Compton form factors for TCS with GPDs obtained from double distribution obtained with MSTW PDFs

$$CFF = LO \quad + \quad NLO \qquad \text{Ratio} = \frac{NLO}{LO}$$

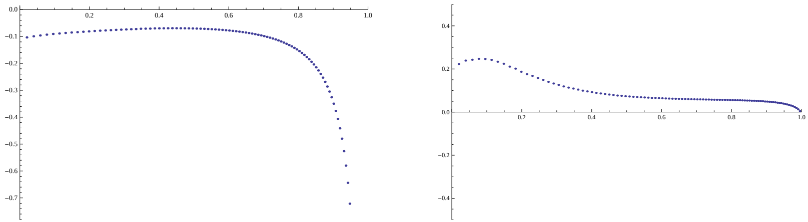

Figure: Ratios of NLO correction to Born contribution for imaginary (left figure) and real (right figure) parts for $Q^2 = 5\text{GeV}^2$, $\mu_F = Q$, $t = 0$

Resummation of large terms

Reminder: INCLUSIVE DIS vs. DY case G. Parisi Phys. Lett. 90B (1980)

$$\sigma^n_{DY} \;=\; \sigma^n_{PM}\; R(\alpha, n)$$

$$R(\alpha, n) \;=\; 1 \;+\; \frac{\alpha(Q^2)}{2\pi} f(n) \;+\; \mathcal{O}(\alpha^2(Q^2))$$

σ^n_{DY} moments in $\tau = Q^2/s$
σ^n_{PM} predictions of naive parton model at $q^2 = -Q^2$

$$f(n) \sim \frac{4}{3}\left(\frac{4}{3}\pi^2 \;+\; 2\ln^2 n\right) \quad \text{for} \;\; n >> 1$$

π^2 terms: analytic continuation from $q^2 < 0$ to $q^2 > 0$
$\ln^2 n$ terms: soft gluons
$\Longrightarrow$ large terms exponentiate into quark e-m. form factor

Resummation of large terms

Reminder: INCLUSIVE DIS vs. DY case G. Parisi Phys. Lett. 90B (1980)

$$\sigma^n_{DY} = \sigma^n_{PM}\, R(\alpha, n)$$

$$R(\alpha, n) = 1 + \frac{\alpha(Q^2)}{2\pi} f(n) + \mathcal{O}(\alpha^2(Q^2))$$

σ^n_{DY} moments in $\tau = Q^2/s$
σ^n_{PM} predictions of naive parton model at $q^2 = -Q^2$

$$f(n) \sim \frac{4}{3}\left(\frac{4}{3}\pi^2 + 2\ln^2 n\right) \quad \text{for} \quad n >> 1$$

π^2 terms: analytic continuation from $q^2 < 0$ to $q^2 > 0$
$\ln^2 n$ terms: soft gluons
$\Longrightarrow$ large terms exponentiate into quark e-m. form factor

Resummation in case of EXCLUSIVE processes:
e.g. DVCS vs. TCS case: no results work in progress

Conclusions of the NLO part:

- new results: NLO corrections to DVCS, TCS and to DDVCS
- corrections seem to be big ...
- better understanding of large terms (π^2, ??) is needed resummation
- realistic phenomenology needed: (in progress)
  - realistic GPD convoluted with our NLO CFs
  - calculation of relevant observables

- NICE DATA FROM LHC, RHIC and JLab ON TCS, DDVCS ARE VERY NEEDED !!

THANK YOU FOR YOUR ATTENTION